Int. J. Adv. Sci. Eng.
Vol. 1 No. 4 1-9 (2015) 1 *ISSN 2349 5359*

RESEARCH ARTICLE

Experimental and quantum chemical study on geometry, stability, electronic structures, electronic Absorption, solvents effect and efficiency of β,ε-carotene-3,3'-diol as Natural Sensitizers for Dye Sensitized Solar Cells

K. Suguna[a], P.B. Nagabalasubramanian[b*], P.M. Anbarasan[c], R. Rengaiyan[b]

[a]Department of Physics, Periyar University, Salem, Tamil Nadu, India.
[b]Department of Physics, Arignar Anna Govt. Arts & Science College, Karaikal, Puducherry, India.
[c]Centre for Nanoscience and Nanotechnology, Periyar University, Salem, Tamil Nadu, India.

ABSTRACT: β,ε-carotene-3,3'-diol (Lutein) extracted from the leaves of Murraya Koeniggi was subjected to acetone, ethanol and methanol and the effect of solvents on the efficiency of Natural Dye Sensitized Solar Cells (NDSSC) were discussed using UV-VIS, FTIR, and FESEM techniques. DSSC fabrication procedure has been employed using these natural dyes as natural sensitizer of TiO_2 films. DFT and TD-DFT computations were carried out to study and compare the HOMO-LUMO energy gaps and MEP. The HOMO-LUMO energy of the dye, together with the energies of the valence and conduction band edges for TiO_2 and the redox level of the I^-/I_3^- electrolyte are compared.The effect of polar aprotic and protic solvents used in the sensitization process was investigated for the improvement in conversion efficiency of a cell. The overall solar energy conversion efficiencies were obtained as 0.70%, 0.65% and 0.59% for the dye extracted in acetone, ethanol and methanol respectively.

KEY WORDS: Lutein; Natural Dye Sensitized Solar Cells; UV-Vis; β,ε-carotene-3,3'-diol; Murraya Koeniggi;

1. INTRODUCTION

The DSSC is one of the photochemical electric cells, which consists of the photoelectrode, the dye, the electrolyte, and the counter electrode. The energy gap size of the applied semiconductors determines the absorption frequency of light in the solar cells. A significant purpose for using the dyes in the DSSC is to expand the absorption spectra on the visible light. This article provides some experimental data for analyzing the dye's absorption spectra extracted using various solvents, which can be applied in the DSSC.

Solar cells are devices that utilize energy from the sun by converting solar radiation directly into electricity. The conventional solar cell device is silicon-based solar cells with efficiency as high as 30% under concentrated light. However, high manufacturing cost prevents the widespread use of silicon cells [1,2]. NDSSC is a relatively new class of low-cost solar cell. This cell was developed by Gratzel and co-workers as a practicable device which is an interesting field of research at present [3]. In NDSSCs, the dye as a sensitizer plays a key role in absorbing sunlight and transforming solar energy into electric energy. Numerous metal complexes and organic dyes have been synthesized and utilized as sensitizers. By far, the highest efficiency of DSSCs sensitized by Ru-containing compounds absorbed on nanocrystalline TiO_2 reached 11–12% [4,5]. However, these dyes use metal compound complexes, which are expensive and produce environmental pollution [6]. Natural dyes extracted from fruits, flowers and leaves of plants have several advantages such as environment friendly, nontoxic, biodegradable, readily available, easy to extract, no need of further purification and cheaper over rare metal complexes, synthetic and other organic dyes [7]. Natural pigments, including chlorophyll, anthocyanin [8-13], nasunin [14] carotenoids[15], crocetin [16], Red Indian Spinach [17] are freely available in plant leaves, flowers, and fruits and have the potential to be used as sensitizers.

Up to now, carotenoids have been not much paid attention as sensitizers for the NDSSCs for two reasons. First, most carotenoid species do not have effective functional group to bond with –OH of TiO_2.Secondly, strong steric hindrance of long chain alkane of carotenoid species prevents the dye molecules from arraying on TiO_2 film efficiently [18]. Due to these reasons, carotenoid species are not nearly adsorbed on TiO_2 film and sensitizing effect on TiO_2 film tends to be low. However, Lutein, a carotenoid with hydroxyl groups in the molecule exhibited a high binding ability to the surface of TiO_2 semiconductor film. Lutein is a Xanthophyll and one of known naturally occurring carotenoids. The principal natural stereoisomer of Lutein is (3R,3'R,6'R)-beta,epsilon-carotene-3,3'-diol. Lutein is a lipiphilic molecule and is generally insoluble in water. The presence of the long chromophore of conjugated double bonds (polyene chain) provides the distinctive light absorbing properties.

So, in this paper, extracts of Murraya Koenigii leaves (Lutein- β,ε-carotene-3,3'-diol) using various solvents were prepared and the effect of extracting solvents on the efficiency of NDSSCs were discussed using UV-VIS Spectroscopy, FTIR, and FESEM techniques. Besides, the quantum chemical calculations are utilized to interpret the electronic properties of the dye molecule. The energy of the

**Corresponding author*
ekrubha@yahoo.com

Received : 10.03.2015
Accepted : 25.04.2015
Published on: 20.05.2015

HOMO and LUMO molecular orbitals of the dyes, together with the energies of the valence (VB) and conduction (CB) band edges for TiO_2 and the redox level of the I^-/I_3^- electrolyte are compared. Further, the extracted dyes are mixed with the solvents of acetone, ethanol and methanol were employed as natural sensitizers in the fabrication of NDSSCs and the photo-electro-chemical performances of these cells were investigated.

2. EXPERIMENTAL PROCEDURES

2.1. Preparation of Natural Dye Sensitizer Solution

Fresh curry leaves each of 10 g (3 samples) were separately weighed on an electronic weighing balance and crushed with a porcelain mortar and pestle, each crushed sample was then mixed with 50 ml of ethanol, methanol and acetone (99% absolute) at room temperature. The samples covered with Aluminium foil were kept in a dark room. After 24 hours, solid dregs in the solution were filtered out to acquire a pure and clear dye solution. Intentionally, any further purification of the extracts was avoided to check whether an efficient sensitization could be achieved with minimal chemical process. The natural dye solutions were protected from direct light exposure.

2.2. Preparation of TiO2 Electrode and Counter Electrode

The conducting glass substrate (FTO of 2.5 x 2.5 cm2, Solaronix, Switzerland) was immersed in isopropanol for 48 hrs to remove any impurities. Then the glass plates were first cleaned using an ultrasonic bath with acetone, ethanol, and water for about 10 min each. To prepare TiO_2 colloidal solution, the TiO_2 (P25 Degussa, Sigma-Aldrich, India) powder was grinded with 5 ml of distilled water and Acetyl acetone of 0.1ml for 30 minutes in an agate mortar. Finally alcohol of 1.0 ml containing emulsification agent (octylphenylether polyethylene glycol) of 0.1 ml was slowly added with grinding continuously for the other 30 min. A Scotch tape at four sides was used as masking material on the conductive layer of the FTO glass plate to restrict the thickness and area of the paste (1 cm x 1 cm). The TiO_2 paste was then coated on the FTO plate using the doctor blade method. Later the glass is sintered at 450°C for 60 minutes under thermal furnace module to solidify TiO_2 on [19]. After the annealing process, when the temperature of the film paste drops to 80°–90°C [20], the coated glasses were immersed into natural dye solutions and left for 24 hours to absorb the dye on TiO_2 porous film adequately. Excess non-adsorbed dye were washed using with anhydrous ethanol. In order to ascertain the effect of organic solvents, polar aprotic solvent acetone, polar protic solvent ethanol and methanol were used in the extraction of the natural dye.

The counter electrode i.e., platinum electrode was prepared from Pt (Plastisol, Solaronix, Switzerland) by spreading a few drops on the FTO glass, followed by drying at 100°C for 10 minutes and then at 385°C for 30 minutes [21].

2.3. Dye Sensitized Solar Cell Assembly

DSSCs were assembled following the procedure described in the literature [22], the catalyst-coated counter electrode was placed on the top so that the conductive side of the counter electrode faces the TiO_2 film. Two binder clips were used to hold the electrodes together. The iodide electrolyte solution was placed at the edges of the plates. The liquid was drawn into the space between the electrodes by capillary action. This resulted in the formation of sandwich type cell.

2.4. Characterization and Measurement

Structural characterization was carried out by X-ray diffraction using (SHIMADZU-6000 Model) X-ray Diffractometer. The morphological features of the samples were also observed using the scanning electron microscope (SEM; Quanta200 FEG). Roughness of the thin films prepared was analyzed using Atomic Force Microscope (Veeco). Perkin Elmer System one FT-IR Spectrometer was used to measure FTIR spectra. UV–VIS absorption spectra of natural dyes were recorded using Lambda 35 Perkin Elmer UV-Vis Spectrophotometer. The photovoltaic property was carried out by measuring the I–V character curves under standard illumination conditions (Sol3A Class AAA Solar Simulator) in ambient atmosphere. Solar cell characterization was done with a standard solar spectrum of air mass 1.5 (AM 1.5) with an intensity of 1000 W/m^2 [23]

2.5. Theoretical Computational Methods

The foremost task for the computational work is to determine the optimized geometry of the compound. The molecular structure optimization of the title compound are calculated using DFT with hybrid Beckee-3-Lee-Yag-Parr (B3LYP) combined with 3-21G basis set using GAUSSIAN 09 program package [24] without any constraint on the geometry. By combining the results of the GAUSSVIEW program [25] with symmetry considerations, vibrational frequency assignments were made with a high degree of accuracy. The HOMO-LUMO energies, energy gap are calculated with the same basis set. The MEPs, total density and contour of the present molecule is analyzed.

3. RESULTS AND DISCUSSION

3.1. Optimized geometrical structure of BEC33'D

The molecular structure along with numbering of atoms of β,ε-carotene-3,3'-diol abbreviated as BEC33'D (lutein) is obtained from Gaussian 09 and GAUSSVIEW programs and is as shown in the Fig.1. The global minimum energy obtained by DFT structure optimization using 3-21 G basis set for the title molecule as -1698.9872 a.u.

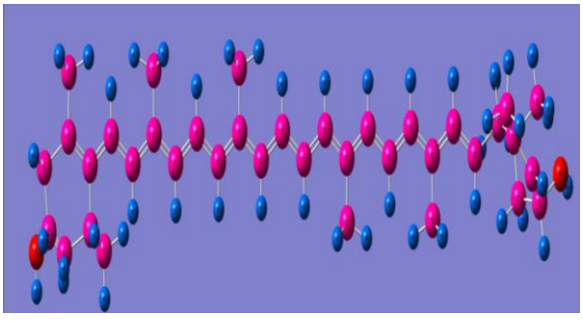

Fig.1. Optimized Geometrical Structure of BEC33'D (Lutein) using B3LYP/3-21G Basis set

3.2. Crystal structure of TiO_2

Fig.2 shows the XRD patterns of the sample TiO_2 annealed in air at 450 °C. TiO_2 can be assigned to anatase crystal phase according to the standard XRD patterns. The peaks at 25.32º is assigned to the (101) lattice planes, which are attributed to the signals of the anatase phase. All diffraction peaks were assigned to pure anatase phase [26] without other crystalline by-products. Moreover, the peaks are rather sharp, which indicates that the obtained TiO_2 has relatively high crystallinity.

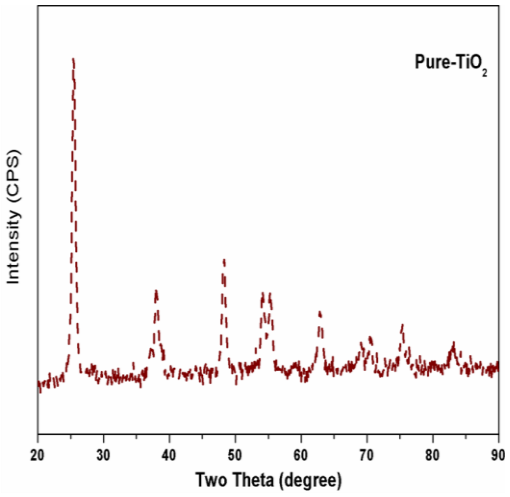

Fig.2. XRD structure of BEC33'D (Lutein)

3.3. FTIR spectral Analysis

The experimental FTIR spectra of extracted dyes from BEC33'D in three solvents viz., acetone, ethanol and methanol are as shown in Fig.3. The peaks at 1068 cm^{-1} of the dye extracted in solvent acetone, 1089 $cm^{-1}$and 1049 cm^{-1} in ethanol and 1027 cm^{-1} in methanol were assigned to C-C stretching vibrations. The peaks at 1697 cm^{-1}, 1646 cm^{-1}, 1424 cm^{-1} in acetone, 1654 cm^{-1}, 1453 cm^{-1}, 1420 cm^{-1} in ethanol and 1657 cm^{-1}, 1449 cm^{-1}, 1420 cm^{-1} in methanol are attributed to the symmetric vibrational modes of C=C stretching. These are important spectroscopic measurements since they reflect the structural properties of the carotenoid molecule [27]. The strong and broad band's at 3412 cm^{-1}, 3369 cm^{-1} and 3367 cm^{-1} in acetone, ethanol and methanol respectively are due to the –OH vibrations. The peaks at 2975 cm^{-1}, 2928 cm^{-1} and 2895 cm^{-1} in ethanol and 2946 cm^{-1} and 2834 cm^{-1} in methanol correspond to the –CH stretching mode [28, 29].

The peaks at 1238 cm^{-1}, 1274 cm^{-1} are due to the presence of C-O stretching vibrations. The bands due to C–H in-plane ring vibration interacting somewhat with C–C stretching vibration are observed as a number of m–w intensity sharp bands in the region 1000–1300 cm^{-1}. In this study, the FT-IR peaks at 1370 cm^{-1}, 1381cm^{-1}, 1329 cm^{-1} were assigned to C–H in-plane-bending vibrations as reported in Table.1. In line with the earlier literatures [30, 31], the wave numbers in the region between 880 cm^{-1} to 629 cm^{-1} are assigned to CH out of plane bending vibrations.

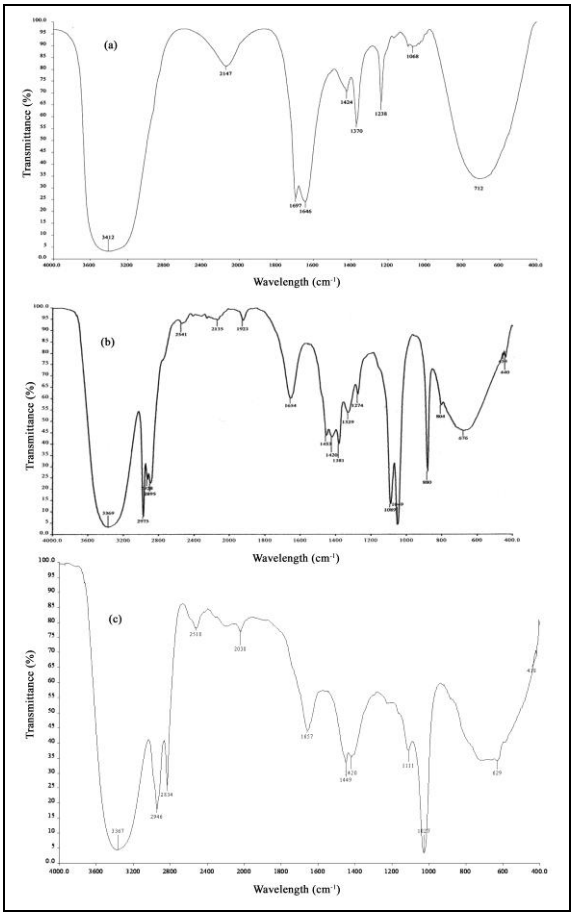

Fig.3.Experimental FTIR Spectrum of lutein (BEC33'D) in (a) acetone, (b) ethanol and (c) methanol

3.4. UV-VIS Spectroscopic Analysis

The Experimental UV-Vis absorption spectra of BEC33'D at different solvents such as acetone, ethanol and methanol are as shown in Fig.4. The absorption wavelength in three different solvents was shown in Table 2. As can be seen from the table 2, the experimental absorption maxima were observed at 422.31 nm, 536.11 nm, 607.77 nm and 664.24 nm in acetone. In ethanol, the maximum absorption peaks were observed at 440.97 nm, 473.99 nm, 625.33nm and 674.65 nm. In methanol, the absorption maxima were observed at 411.56 nm, 421.97 nm, 535.04 nm, 609.15 nm and 664.17 nm.

The main absorption range of N719 is in 400–600 nm; the absorption range of lutein dye is in 400–500 nm and in 600–750 nm. Hence, lutein dye's absorbability is better in the range of 400–450 nm. But in the range of 500– 600 nm, N719's absorbability is better than that of lutein dye. The spectrum obtained between 400 and 500 nm confirms the extraction of the carotenoid pigment.

The absorbance intensity of the lutein with acetone (536.11 nm) was very high compared to that of ethanol (473.99 nm) and methanol (535.04 nm). It appears that selection of the appropriate solvent plays a role in improving the efficiency of a cell by virtue of enhancing microphase separation resulting amphiphilicity toward more dye adsorption. The

polar aprotic solvent such as acetone was found to be more effective for dye diffusion, whereas ethanol and methanol being polar protic in nature was not suitable for dye diffusion.

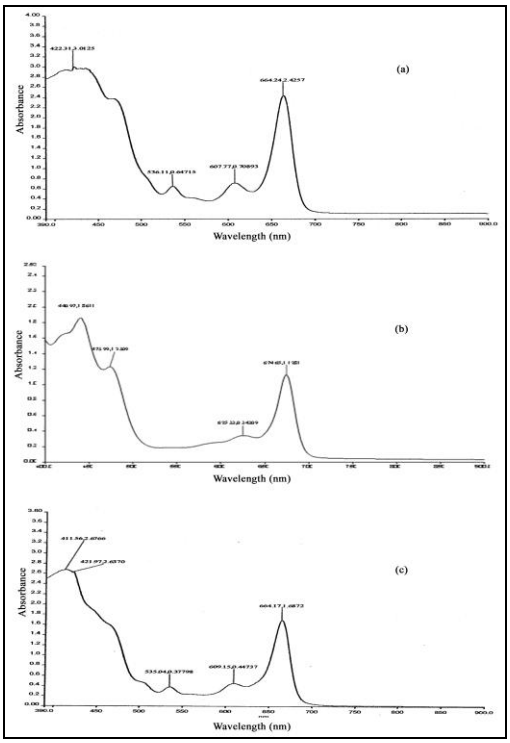

Fig.4.Experimental UV-Vis Spectrum of BEC33'D in (a) acetone, (b) ethanol and (c) methanol

Table 2 Experimentally calculated wavelengths λ (nm) absorbance and energy(eV) BEC33'D of in three different solvents

Solvent	λ (nm)	Absorbance	Energy (eV)
ACETONE	422.3	3.0125	2.9358
	536.1	0.6472	2.3126
	607.8	0.7089	2.0399
	664.2	2.4257	1.8665
ETHANOL	441	1.8611	2.8115
	474	1.2309	2.6157
	625.3	0.3431	1.9826
	674.7	1.1281	1.8377
METHANOL	411.6	2.6766	3.0124
	422	2.637	2.9381
	535	0.378	2.3172
	609.2	0.4474	2.0353
	664.2	1.6872	1.8667

3.5. HOMO – LUMO energy levels

The Frontier energy level diagrams (HOMO and LUMO) of the pigment obtained from DFT/B3LYP/3-21G method is as shown in Fig.5. The electronic transition from ground state to first excited state is mainly explained by one electron excitation from HOMO to LUMO. The HOMO represents the ability to donate an electron, LUMO as an electron acceptor, represents the ability to obtain an electron. The energy of HOMO is directly related to ionization potential and LUMO energy is directly related to electron affinity. These orbitals determine the way in which the molecule interacts with other species. The frontier molecular orbital energy gap helps to characterize the chemical reactivity and kinetic stability of the molecule. A molecule with a smaller energy gap between HOMO–LUMO is more polarizable, with high chemical reactivity and low kinetic stability.

The 3D FMOs plots of the pigment in Fig.5 implied that the positive and negative phases are represented by red and green color respectively. For efficient injection of the electron of the excited dye into the metal oxide semiconductor e.g. TiO_2, the LUMO level of the dye needs to be higher than the conduction band edge of the semiconductor [32, 33]. The band edge of TiO_2 is approximately at - 4.2 eV (relative to vacuum) [34] and the LUMO energy level of BEC33'D is - 2.186 eV. Hence, Fig.5 indicating that the LUMO levels of the dye is higher than the conduction band edge of TiO_2.

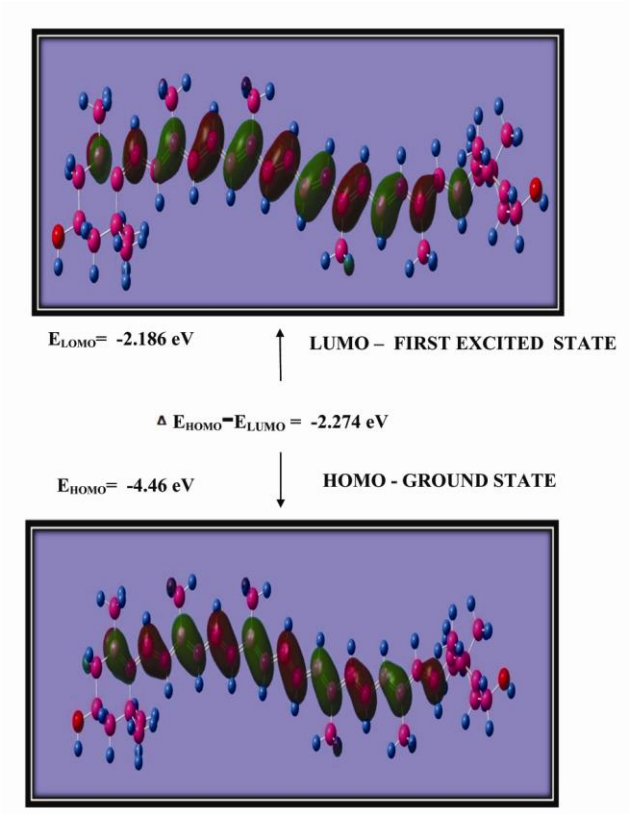

Fig.5. Isodensity plots of the frontier orbitals of the dye BEC33'D and corresponding orbital energies

The HOMO level of the dye needs to be sufficiently lower than the redox couple to ensure the efficient regeneration of the dye [32]. The most widely used redox couple in the electrolyte of DSSC is the I^-/I_3^- pairs where the estimated energy level is at - 4.8 eV (relative to vacuum) [33]. The HOMO of BEC33'D is - 4.46 eV, which is more negative than the energy level of the redox couple.

Hence, from the above results it is clear that the LUMO lies above the conduction band edge of TiO_2, making possible the transfer of the photoelectron from the dye to the semiconducting oxide. Also, the HOMO of all dyes lies below the redox level of the electrolyte, allowing for the transfer of the electron to the pigment and its regeneration.

3.6. FESEM Analysis

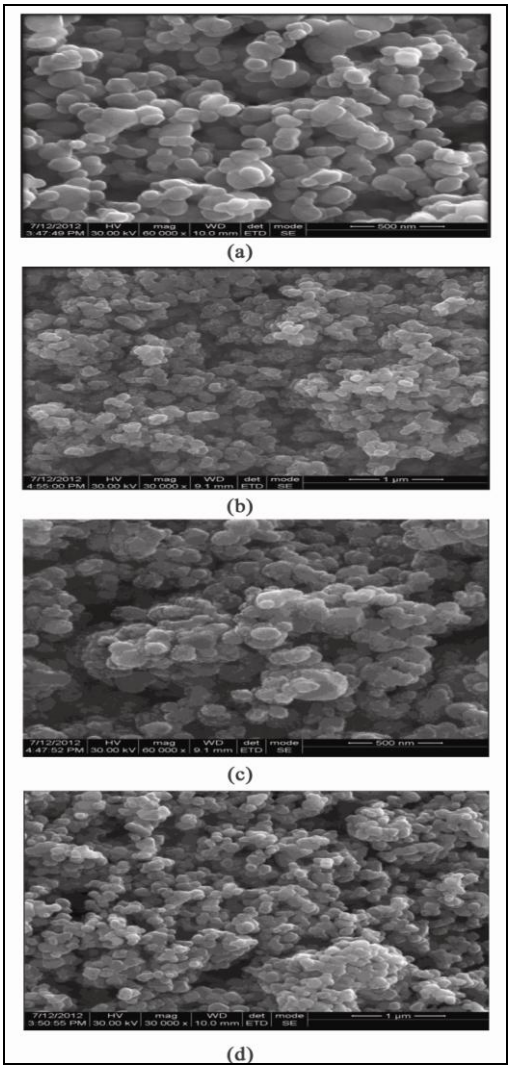

Fig.6. (a) SEM picture Pure-TiO_2 film; (b) SEM picture of BEC33'D in acetone on TiO_2 film; (c) SEM picture of BEC33'D in ethanol on TiO_2 film; and (d) SEM picture of BEC33'D in methanol on TiO_2 film

Fig.6 (a) shows the scanning electron micrograph of a typical TiO_2 (anatase) film deposited by doctor blade technique on a conducting glass sheet (FTO) that serves as current collector. Analysis of the layer morphology shows the porosity to be about 50–65%, the average pore size being 70 nm. The SEM image indicates that the TiO_2 particles were spherical in shape and composed with a high degree of porosity which may help to improve adsorption of dye molecules on the surface. The porous structure of the (a) film enlarges the surface area greatly, up to a factor of 1000 as compared to a flat surface, which facilitates the dye adsorption loading and also enables light harvesting due to its reflective nature [35]. The Fig.6 (b), (c) and (d) shows the Scanning electron microscope pictures of TiO_2 with the adsorption of the dye BEC33'D extracted in solvents acetone, ethanol and methanol respectively. In a sharp contrast with the (a) film, the other films have a dense and flat surface, as well as a compact internal structure with an average particle size of 70 to 80 nm. By comparing the figures, there are more adsorption with the acetone solvent than other solvents ethanol and methanol.

3.7. AFM Analysis

The AFM images of the prepared pure TiO_2 film and dye (extracted in acetone) coated TiO_2 which are shown in figures 7(a) and 7(b) respectively. Root-mean-square (RMS) height is defined as the mean of the root for the deviation from the standard surface to the indicated surface. The high RMS means high surface roughness. The calculated RMS roughness values are 70.49 nm and 54.21 nm for pure TiO_2 and dye (in acetone) adsorbed TiO_2 respectively. When the dye was adsorbed on to the semiconductor, the RMS roughness value found to be decreased. This reduction in roughness was attributed to the smoothing effect induced by the dye molecules as it fills exactly the gaps between the TiO_2 nano particles. This means that there is more favourable cluster formation in P25 TiO_2 films in the presence of sensitizer [36].

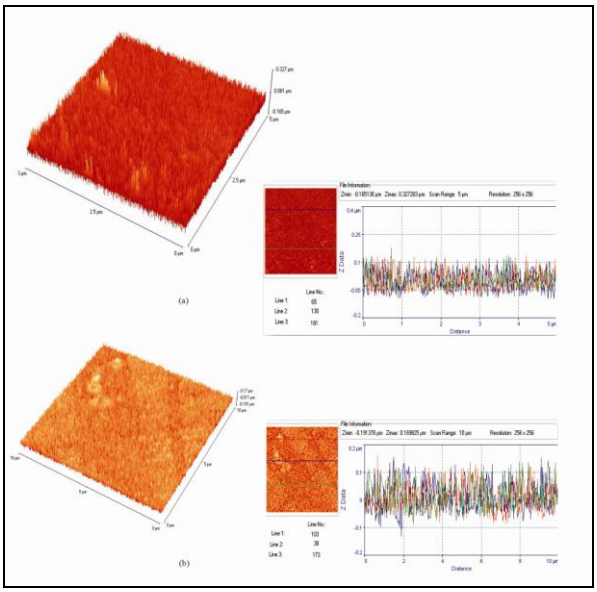

Fig.7. (a) AFM picture of TiO_2 film; (b) AFM picture of TiO_2 film coated with dye

3.8. Molecular Electrostatic Potential

In order to understand the MEPs of BEC33'D molecule, it is plotted in 3D and given in Fig.8(a) using DFT/ B3LYP method 3-21G basis set in gas phase. The MEPs is a plot of electrostatic potential mapped onto the constant electron density surface. The MEPs superimposed on top of the total energy density as a shell. Because of the usefulness feature to study reactivity given that an approaching electrophile will be attracted to negative regions (where the electron distribution effect is dominant). In the majority of the MEPs, while the maximum negative region which preferred site for electrophilic attack indications as red color, the maximum positive region which preferred site for nucleophilic attack symptoms as blue color. The importance of MEPs lies in the fact that it simultaneously displays molecular size, shape as well as positive, negative and neutral electrostatic potential regions in terms of colour grading and is very useful in research of molecular structure with its physicochemical property relationship [37, 38].

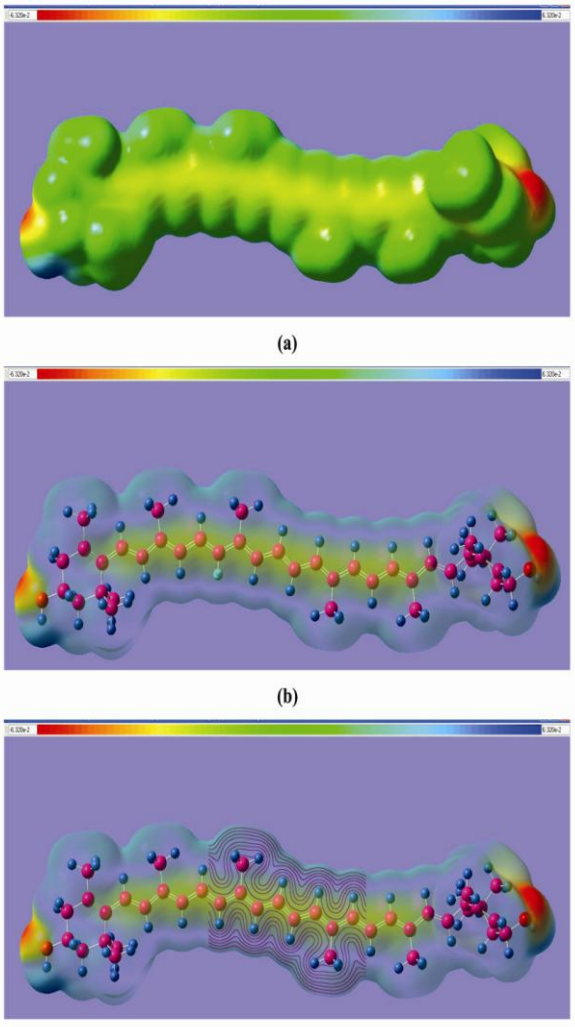

Fig.8. (a) Electron density (b) Molecular Electrostatic potential (c) Contour of BEC33'D in gas phase using B3LYP/3-21G basis set

It is clear from the analysis that the dye acetone was more efficient than in the other solvents. This is because the According to the MEPs of the title molecule in 3D plots (fig. 8(b)), the different values of the electrostatic potential at the surface are represented by different colours in the map of MEPs. The potential increases in the order from red to blue color. The colour code of the maps is in the range between -6.320e^{-2} (dark red) and +6.320e^{-2} (dark blue) in compound, where blue indicates the strongest attraction and red indicates the strongest repulsion. As can be seen from the MEPs map of BEC33'D molecule, there are more region having the less positive potential (light blue) around the hydrogen atoms of the molecule, but there is the negative potential around the oxygen atom of OH group at the two ends of the molecule. As a result, the molecule has no strongest attraction but, has the strongest repulsion (see figure 8(b)).

3.9. Photo-electrochemistry of DSSC

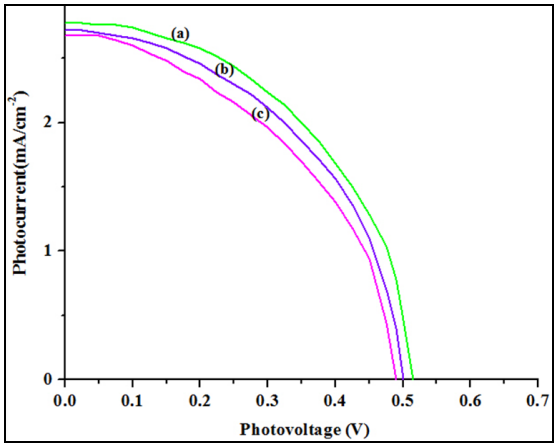

Fig.9. I-V characteristics of DSSCs sensitized with Murraya Koeniggi (lutein) leaves extracted in solvent (a) acetone, (b) ethanol and (c) methanol

Fig.9 shows the I-V curve of the prepared NDSSC that takes Murraya Koeniggi leaves extracted in different solvents as natural sensitizers. Furthermore, Table.3 compares the different property parameters of DSSCs, including short circuit photocurrent density (I_{sc}), open circuit voltage (V_{oc}), fill factor (FF) and energy conversion efficiency (η). The η of the Lutein in solvent acetone sensitized solar cell was 0.70 % with short circuit current density 2.78 mA/cm^2, open circuit voltage 0.515 V and fill factor 0.49; while the η of the sensitizer in solvent ethanol was 0.65 % with I_{sc} 2.72 mA/cm^2, V_{oc} 0.50 V and FF 0.48. The η of the Lutein in solvent methanol sensitized solar cell was 0.59% with short circuit current density 2.68 mA/cm^2, open circuit voltage 0.49 V and fill factor 0.45. The TiO_2 spheres usually possess high specific surface area which results in better photocatalytic performance because the photocatalytic reactions are based on chemical reactions on the surface of the photocatalyst. These structural features increase the light-harvesting capabilities of these materials because they enhance light use by allowing as much light as possible to access the interior [39].

density of the dye molecule adsorbed to the TiO_2 electrode was greater in the presence of acetone. This is because

during sensitization in the acetone solvent, the HOMO–LUMO gap was found to be comparatively narrower than other solvents, which leads to easier excitation and the subsequent injection process.

Table 3 Photo-electrochemical parameters of DSSCs sensitized with BEC33'D in three different solvents

Solvent	I_{sc} (mA/cm²)	V_{oc} (V)	FF	η (%)
Acetone	2.78	0.52	0.49	0.7
Ethanol	2.72	0.5	0.48	0.65
Methanol	2.68	0.49	0.45	0.59

Solar cells prepared using natural dye extracted in acetone shows a higher efficiency than that of solar cells prepared using natural dye extracted in ethanol and methanol. This may due to the higher solubility of carotenoids in acetone and hence the aggregation of dye molecules is less as expected [40]. A good dispersion of dye molecules on the oxide surface could in fact improve the efficiency of the system. Hence, dyes extracted using acetone shows good adsorption on the working electrode. The higher cell efficiency of the dye extracted in solvent acetone comes from enhanced open circuit voltage and short circuit current density as seen from the Table 3.

4. CONCLUSION

NDSSCs have been fabricated using Murraya Koeniggi leaves dye extracted in solvents acetone, ethanol and methanol as natural sensitizers. The peaks at around 1070 cm^{-1} and 1640 cm^{-1} for the carotenoid molecule are attributed to the symmetric vibrational mode of the C-C and C=C stretching. The leaves are characterised by good absorption spectrum between 400 nm to 700 nm when extracted in solvents acetone, ethanol and methanol. In UV spectra the light absorption in the range 400-670 nm make carotenoids potential sensitizer materials for DSSCs. FESEM and AFM studies support the capability of the dye as sensitizer.

The overall conversion efficiency of the cells using dyes extracted in solvents of acetone, ethanol and methanol line up as 0.70, 0.65 and 0.59 % respectively. From the above result it was observed that the efficiencies are less than 1%. The main reason for the low efficiencies of natural dyes is due to the structure of the pigments. The structure of Lutein has long chain which hinder the bonding of the pigment with the oxide surface of the TiO_2, thus preventing the dye molecule to move to the conduction band of TiO_2. However the short circuit current, open circuit voltage and efficiency are higher in the cells prepared using the dye extracted in solvent acetone. This may be due to the higher concentration of the dye molecules in acetone. In the aprotic solvent (acetone) extract, the concentration of Lutein is expected to be higher than in protic solvents (ethanol and methanol), probably because of higher solubility in acetone which leads to less aggregation and significant dispersion of the dye molecules.

The optimized geometrical structure and the HOMO, LUMO energies of BEC33'D (Lutein) were calculated using B3LYP/3-21G Basis set. The calculated HOMO energy was -4.46 eV whereas the LUMO energy was -2.186 eV. The HOMO – LUMO energy gap was calculated as 2.274 eV. The theoretically calculated HOMO value was compared with the redox potential and the LUMO value is compared with the experimentally calculated conduction band of TiO_2. This comparison implies that there will be charge transfer takes place within the molecule and it should be used for NDSSC applications.

Table 1 Experimental FT-IR frequency of BEC33'D calculated in three different solvents

Experimental frequency (cm^{-1}) in solvents					
Acetone	**Vibrational assignments**	**Ethanol**	**Vibrational assignments**	**Methanol**	**Vibrational assignments**
3412	ν O–H	3369	ν O–H	3367	ν O–H
2147	-------	2975	ν X–H	2946	ν X–H
1697	ν X=X	2928	ν X–H	2834	ν X–H
1646	ν X=X	2895	ν X–H	2518	------
1424	ν X=X	2541	-------	2038	------
1370	β C-H	2135	-------	1657	ν X=X
1238	ν X–O	1923	-------	1449	ν X=X
1068	ν X–X	1654	ν X=X	1420	ν X=X
712	γ C-H	1453	ν X=X	1111	-------
		1420	ν X=X	1027	ν X–X
		1381	β C-H	629	γ C-H
		1274	ν X–O		
		1089	ν X–X		
		1049	ν X–X		
		880	γ C-H		
		804	γ C-H		
		676	γ C-H		

REFERENCES

1. Li, B. , Wang, L., Kang, B., Wang, P., Qiu,Y., 2006, Review of recent progress in solid-state-dye-sensitized solar cells, Solar Energy Materials & Solar Cells, 90(5), 549
2. Smestad, G.P., 1998, Education and solar conversion: Demonstrating electron transfer, Solar Energy Materials & Solar Cells, 55, 157.
3. Regan,B.O., Gratzel, M., 1991, A low-cost, high-efficiency solar cell based on dye-sensitized colloidal TiO2films, Nature, 353, 737.
4. Chiba, Y., Islam, A., Watanabe, Y., Komiya, R., Koide, N., Han, L.Y., 2006, Dye-sensitised solar cells with conversion efficiency of 11.1%, J. Appl. Phys., 45,638.
5. Buscaino, R., Baiocchi, C., Barolo, C., Medana, C., Gratzel, M., Nazeeruddin,K., 2008, A mass spectrometric analysis of sensitizer solution used for dye-sensitized solar cell. Inorganica Chimica Acta, 361,1584-1596.
6. Chang, H., Wu, H. M., Chen, T. L., Huang, K. D., Jwo, C. S., Lo, Y. J., 2010, Dye sensitized solar cell using natural dyes extracted from spinach and ipomoea, Journal of Alloys and Compounds, 495, 606.
7. Patrocínio, A. O. T., Mizoguchi, S. K., Paterno, L. G., Garcia, C. G., Iha, N. Y. M., 2009, Efficient and low cost devices for solar energy conversion: Efficiency and stability of some natural-dye-sensitized solar cells , Synthetic Metals, 159, 2342.
8. Hao, S., Wu, JH., Huang, Y., Lin, 2006, Natural dyes as photo sensitizers for dye sensitized solar cell J.Sol Energy, 80,209.
9. Dai Q, Rabani J., 2001, Photosensitization of nanocrystalline TiO2 films by pomegranate pigments with unusually high efficiency in aqueous medium, Chem Commun., 20, 2142.
10. Cherepy, NJ., Smestad, GP., Gratzel, M., Zhang, JZ., 2006, Ultrafast Electron Injection: Implications for a Photoelectrochemical Cell Utilizing an Anthocyanin Dye-Sensitized TiO2 Nanocrystalline Electrode, J Phys Chem. B, 997,9342.
11. Wongcharee, K., Meeyoo, V., Chavadej, S., 2007, Dye-Sensitized Solar Cell Using Natural Dyes Extracted from Rosella and Blue Pea Flowers, Sol Energy Mater & Solar Cells, 91,566.
12. Chapbell, WM., Jolley, KW, Wagner, P., Wagner, K., Walsh, P., Gordon, KC., Mende, LS., Nazeeruddin, MK., Wang, Q., Gratzel, M., Officer, DL, 2007, Highly Efficient Porphyrin Sensitizers for Dye-Sensitized Solar Cells, J. Phys. Chem. C, 111,11760.
13. Calogero Giuseppe, Di Marco Gaetano., 2008, Red Sicilian orange and purple eggplant fruits as natural sensitizers for dye-sensitized solar cells. Solar Energy Mater. & Solar Cells, 92, 1341.
14. Gomez-Ortiz,N.M., Vazquez-Maldonado, I.A., Perez-Espadas, A.R., Mena-Rejon, G.J., Azamar-Barrios, J.A., Oskam, G., 2010, Dye-sensitized solar cells with natural dyes extracted from achiote seeds, Solar Energy Mater. Solar Cells, 94, 40.
15. Yamazaki Eiji, Murayama Masaki, Nishikawa Naomi, Hashimoto Noritsugu, Shoyama Masashi, Kurita Osamu,2007, The dye-sensitized solar cells (DSCs) were assembled by using natural carotenoids, crocetin, Solar Energy, 81,512.
16. Peesole, R.L., Shield, L.D., McWilliam, I.C., Modern Methods of Chemical Analysis, Wiley, New York, 1976.
17. Prabu, K.M., Suguna, K., Anbarasan, P.M., Selvankumar,T., Aroulmoji, V., 2014, Sensitizers performance of Dye-Sensitized Solar Cells fabricated with Indian Fruits and Leaves. Int.J.Adv.Sci.Eng, 1(2), 24.
18. Eiji Yamazaki, Masaki Murayama, Naomi Nishikawa, Noritsugu Hashimoto, Masashi Shoyama, Osamu Kurita, 2007, Utilization of natural carotenoids as photosensitizers for dye-sensitized solar cells. Solar Energy, 81, 512.
19. Larry Lewis, N., 2006, A novel UV-mediated low-temperature sintering of. TiO2 for dye-sensitized solar cells, Solar Energy Materials & Solar Cells, 90, 1041.
20. Matthias Junghänel, Ecole Polytechnique Federale de Lausanne Institute des Sciences et Ingenierie Chimiques, 2007.
21. Longo, C., De Paoli, M.A., 2003, Dye-sensitized solar cells: a successful combination of materials, J.Brazilian Chemical Society, 14, 889.
22. Smestad, G.P.,1998, Education and solar conversion: Demonstrating electron transfer, Solar Energy Materials and Solar Cells, 55,157.
23. Green, M. A., Solar cells. Operating principle, technology and system application, Prentice-Hall, Inc., Englewood Cliffs, 1998.
24. M.J. Frisch, et al., 2003, Gaussian 09, Revision A.1, Gaussian Inc., Pittsburgh, PA, 555.
25. Frisch, A., Nielson, A.B., Holder, A.J., 2000, GAUSSVIEW User Manual, Gaussian Inc., Pittsburgh, PA, 556.
26. Joint Committee on Powder Diffraction, International Centre for Diffraction Data, 2001.
27. Polvka, T., Sundstrom, V., 2004, Ultrafast dynamics of carotenoid excited States-from solution to natural and artificial systems, Chem. Rev., 104,2021.
28. Bunghez, I.R., Raduly, M., Doncea, S., Aksahin, I., Ion, Dig, R.M., 2011, J. Nanomater. Bios., 6, 1349.
29. Lóránd, T., Deli, J.Z., Molnár, P., Tóth, G., 2002, FT-IR study of some Carotenoids, Helvetica Chim. Acta, 85, 1691.
30. Kalsi, P.S., Spectroscopy of Organic Compounds, Wiley Eastern Limited, New Delhi, 1993.
31. Mohan, J., Organic Spectroscopy – Principle and Applications, 2nd ed., Narosa Publishing House, New Delhi, 2005, pp.30.
32. Lee, J.K., Yang, M., 2011, Progress in Light Harvesting and Charge Injection of Dye-Sensitized Solar Cells, Materials Science and Engineering B, 176,1142.
33. Calogero, G., Sinopoli, A., Citro, I., Di Marco, G., Petrov, V., Diniz, A.M., Parola, A.J., Pina, F.,2013, Synthetic analogues of anthocyanins as sensitizers for dye-sensitized solar cells Photochemical and Photobiological Sciences, 12, 883.
34. Heera, T.R., Cindrella, L., 2010, Molecular orbital evaluation of charge flow dynamics in natural pigments based photosensitizers, J. Molecular Modeling, 16, 523.
35. Peng, B., Jungmann, G., Jager, C., Haarer, D., Schmidt, H.W., Thelakkat, M., 2004, Systematic investigation of the role of compact TiO2 layer in solid state dye-sensitized TiO2 solar cells, Coord. Chem. Rev., 248,1479.

36. Brin R. Liwandowski, 2004, Louisiana State University and Agricultural and Mechanical College, 6,41.
37. Murray, J.S., Sen, K., Molecular Electrostatic Potentials, Concepts and Applications, Elsevier, Amsterdam, 1996.
38. Scrocco, E., Tomasi, J., Lowdin, P., Advances in Quantum Chemistry, Academic Press, New York, 1978.
39. Nakata, K., Fujishima, A., 2012, TiO2 photocatalysis: Design and applications, J Photochem. Photobiology C: Photochem. Rev., 13,169.
40. Lapornik, B., Prosek, M., Wondra, A.G.,2005, Comparison of Extracts Prepared from Plant By-Products Using Different Solvents and Extraction Time, J. Food Eng., 71, 214. Z